THE JOURNAL OF PHYSICAL CHEMISTRY Letters

Letter

pubs.acs.org/JPCL

Synchrotron-Based Highest Resolution Terahertz Spectroscopy of the ν_{24} Band System of 1,2-Dithiine ($C_4H_4S_2$): A Candidate for Measuring the Parity Violating Energy Difference between Enantiomers of Chiral Molecules

Sieghard Albert,*[,†] Fabienne Arn,[†] Irina Bolotova,[†] Ziqiu Chen,[†] Csaba Fábri,[†] Guido Grassi,[†] Philippe Lerch,[‡] Martin Quack,*[,†] Georg Seyfang,[†] Alexander Wokaun,[§] and Daniel Zindel[†]

[†]Physical Chemistry, ETH Zurich, CH 8093 Zurich, Switzerland

[‡]Swiss Light Source, PSI Villigen, CH 5232 Villigen, Switzerland

[§]Energy Department, PSI Villigen, CH 5232 Villigen, Switzerland

Supporting Information

ABSTRACT: The chiral C_2 symmetric molecule 1,2-dithiine (1,2-dithia-3,5-hexadiene, $C_4H_4S_2$) has been identified as a possible candidate for measuring the parity violating energy difference between enantiomers. We report here the observation and analysis of the low-frequency fundamental ν_{24} using highest resolution synchrotron-based interferometric Fourier transform infrared (FTIR) spectroscopy in the terahertz range with a band center of ν_0 = 6.95375559 THz ($\tilde{\nu}_0$ = 231.952319 (10) cm^{-1}) and two related hot bands, the $(\nu_{13} + \nu_{24}) \leftarrow \nu_{13}$ band at ν_0 = 6.97256882 THz ($\tilde{\nu}_0$ = 232.579861 (33) cm^{-1}) and the $2\nu_{24} \leftarrow \nu_{24}$ band at ν_0 = 7.01400434 THz ($\tilde{\nu}_0$ = 233.962001 (14) cm^{-1}). This success in the difficult analyses of the THz spectrum of a complex chiral molecule of importance for fundamental tests on molecular parity violation is enabled by the ideal setup of an FTIR experiment of currently unique resolution with the very stable and bright synchrotron radiation at the Swiss Light Source (SLS).

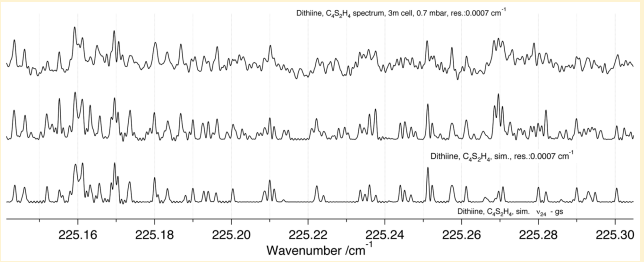

Within the ordinary quantum theory of molecules retaining only the electromagnetic force,[1−3] the enantiomers of chiral molecules are energetically exactly equivalent by symmetry,[4,5] and the ground state would be delocalized with a well-defined parity as part of a tunneling doublet separated by a small splitting $\Delta E_{\pm}$. This would result in a reaction enthalpy $\Delta_R H_0^{\ominus} = 0$ exactly for the stereomutation reaction (eq 1) for localized enantiomers as superposition states of the tunneling doublet states. However, with the discovery of parity violation[6−11] one predicts a small "parity violating" energy difference $\Delta_{pv}E_0$ between the ground states of the two enantiomers as localized eigenstates (provided that $\Delta_{pv}E_0 \gg \Delta E_{\pm}$[4,5]), leading to the prediction of a nonzero parity violating reaction enthalpy $\Delta_{pv}H_0^{\ominus}$

$$\mathrm{P} \rightleftharpoons \mathrm{M} \quad \Delta_{pv}H_0^{\ominus} = N_A \Delta_{pv}E_0 \tag{1}$$

where N_A is the Avogadro constant and we use the P and M notation for "axially chiral" molecules.[12] For a discussion of the consequences for our understanding of the foundations of stereochemistry[5] and possibly also of the evolution of biomolecular homochirality[13−19] as well as a review of theory and the so far unsuccessful experimental attempts to detect molecular parity violation, we refer to the recent reviews[4,20−22] and the literature cited therein. After early erroneous results[23,24](quantitatively incorrect by up to two orders of magnitude for benchmark molecules), theory now seems to converge on consensus.[25−31] However, experimental confirmation or rejection of theory remains a major challenge.[32−40] In this context, it is essential to identify suitable chiral molecules as candidates for experimental tests and to characterize them in preliminary spectroscopic investigations.

We have recently shown[41] that 1,2-dithiine shown in Figure 1 is a potential candidate for measuring $\Delta_{pv}E$ as proposed in refs 33, 39, 40, and 42. The barrier for inversion by ring puckering is ∼2500 cm^{-1} (in wavenumbers), of appropriate magnitude. While the infrared spectra in the higher wavenumber ranges can be partly analyzed on the basis of FTIR spectra using ordinary light sources,[41] the important lowest frequency fundamentals fall in the terahertz range ν = 5 to 8 THz ($\tilde{\nu}$ = 165 to 284 cm^{-1} as summarized in Figure 2), very difficult for traditional FTIR spectroscopy but accessible to highest resolution FTIR spectroscopy using synchrotron light sources as available at the Swiss Light Source (SLS).[43,44] We

Received: July 28, 2016
Accepted: September 8, 2016

DOI: 10.1021/acs.jpclett.6b01674
J. Phys. Chem. Lett. 2016, 7, 3847−3853

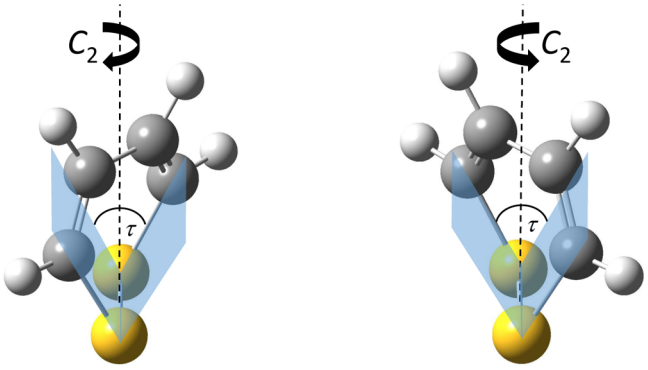

Figure 1. Two enantiomers of 1,2-dithiine ($C_4H_4S_2$, left P, right M enantiomer, following ref 12 for the conventions).

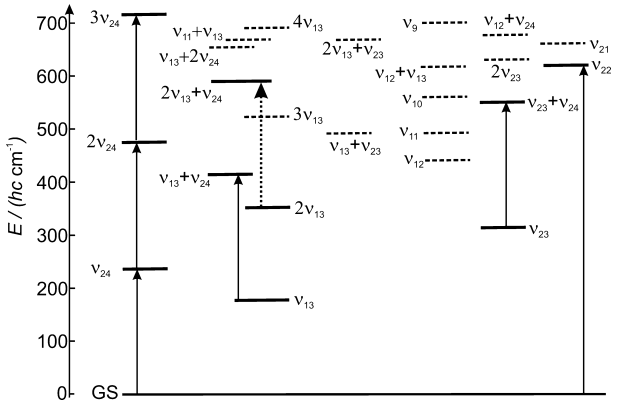

Figure 2. Energy level diagram of 1,2-dithiine ($C_4H_4S_2$) up to 750 cm^{-1}. The solid transitions are experimentally detected; the dashed transitions are calculated.

report here a first successful analysis of the spectra of 1,2-dithiine in this range.

The FTIR spectra of 1,2-dithiine ($C_4H_4S_2$) as synthesized following ref 41 (and refs cited therein) were recorded with the ETHSLS-2009 Bruker prototype[43−46] using synchrotron radiation in the range 200 to 340 cm^{-1}. This prototype spectrometer has a resolution corresponding to an unapodized instrumental bandwidth of 0.00053 cm^{-1} (16 MHz), which is currently the highest for a FTIR spectrometer worldwide. Apertures of 1.8 mm, which allow for an effective instrumental resolution of 0.0006 cm^{-1}, were applied. The sample pressure in a 3 m glass cell at 296 K was 0.8 mbar, excluding substantial pressure broadening. The Doppler width of 1,2-dithiine is 0.00026 cm^{-1} at 230 cm^{-1} and 296 K. The spectra were calibrated with water lines.[47] In general, the calibrated wavenumbers are estimated to be accurate to 0.0001 cm^{-1}. The line data given in the Supporting Information correspond to calibrated wavenumbers.

Figure 3 shows in the upper panel the ν_{24} fundamental spectrum including several hot bands. The lower panels are enlargements within the central Q branch region. Numerous Q branches due to the fundamental and hot bands like the $\nu_{24} \leftarrow$ gs, $(\nu_{13} + \nu_{24}) \leftarrow \nu_{13}$, $2\nu_{24} \leftarrow \nu_{24}$, and $(2\nu_{24} + \nu_{13}) \leftarrow (\nu_{13} + \nu_{24})$ are visible in the middle panel. As one can see in the lower panel of Figure 3, the noise level of the synchrotron spectrum is inferior to about $\lg(I_0/I) = 0.002$, which is 100 times lower than with thermal sources. This low noise level makes it possible to measure the ν_{24} band at high resolution. The use of an effective resolution of 0.0006 cm^{-1} leads to rotationally resolved "eigenstate" lines as the lower panel in Figure 3 illustrates. The decadic absorbance of the weak lines in the spectrum is on the order of only $\lg(I_0/I) = 0.008$. In addition, we have measured rotational transitions in the ν_{24} and ν_{13} vibrational states with our gigahertz setup[41,48] in the range 89 to 108 GHz using a 2.5 m glass cell and sample pressure of ∼0.025 mbar. The frequency is locked to a rubidium standard for short-term stability and to a GPS standard for long-term stability.[41,48]

The equilibrium structure of 1,2-dithiine has C_2 point-group symmetry and the molecular symmetry group M_{S2} (and M_{S4} when including inversion tunneling[4,41]). The nuclear spin statistical weights g of 1,2-dithiine arising from the $2^4 = 16$ nuclear spin functions of the four protons combining with the motional functions to Pauli allowed states correspond for K_aK_c = *ee*:*eo*:*oo*:*oe* to 10:10:6:6 (*e* for even *o* for odd values of the quantum numbers K_a and K_c[49]). 1,2-Dithiine has 24 vibrational modes with symmetry $(n_{\Gamma_v}) = A$ (13 modes) and $(n_{\Gamma_v}) = B$ (11 modes). According to the C_2 symmetry, the modes with A symmetry generate *a*-type transitions, and the modes with B symmetry generate *b*- and *c*-type transitions. In a more detailed description the modes with A symmetry can split into A_1 and A_2 symmetry and the modes with B symmetry into B_1 and B_2 symmetry, as derived for the C_{2v} point group of the planar transition state as reference. As a consequence, the fundamentals with B symmetry generate mainly *c*-type transitions and weak *b*-type transitions if they correspond to "out-of-plane modes" in the planar transition state (B_1) or stronger *b*-type transitions than *c*-type transitions if they correspond to "in-plane modes" (B_2).

Harmonic frequencies, integrated absorption coefficients (corresponding to the double harmonic approximation), and anharmonic energy levels were calculated by the Gaussian 09 program package[50] at the MP2/cc-pVTZ and B3LYP/cc-pVTZ levels of theory and are listed in the Supporting Information. The B3LYP results agree better with experiment than the MP2 results for the four by now known fundamentals, but in any case the results from the two methods indicate the general uncertainties of theories at these levels. We have also calculated the electric dipole transition moment components μ_a, μ_b, and μ_c for the vibrational fundamentals in order to assist the assignments. The ν_{24} mode has been predicted to have a relatively high integrated absorption coefficient of ∼12.0 km mol^{-1}.[41] The anharmonic constants defined by the matrix elements (X_{ij})[49] were used to estimate some selected hot band transitions and their shifts from the ν_{24} fundamental transition.

The infrared spectral region between 200 and 300 cm^{-1} illustrated in Figure 3 shows three major strong absorption features associated with the Q branches of the ν_{24} fundamental, of the hot band $2\nu_{24} \leftarrow \nu_{24}$, and of a third band which we assign as $(\nu_{13} + \nu_{24}) \leftarrow \nu_{13}$. Figure 2 illustrates the vibrational level diagram of the lower energy region. Transitions in this energy range include 25 vibrational fundamental, combination, and overtone states (see Figure 2). The strong sharp lines visible in Figure 3 are due to water absorption lines. In the following description the term "subband" or "series" describes the transitions belonging to one K_a or K_c value. The assignment of the observed rovibrational transitions belonging to a particular subband consisting of P and R branches has been carried out with an interactive Loomis−Wood (LW) assignment program.[49,51,52]

The ν_{24} band of 1,2-dithiine centered at 231.95 cm^{-1} (Figure 3) consists of *c*- and *b*-type transitions. The *c*- and *b*-type transitions are not split for $K_c \leq 7$. The *c*- and *b*-type series were

DOI: 10.1021/acs.jpclett.6b01674
J. Phys. Chem. Lett. 2016, 7, 3847−3853

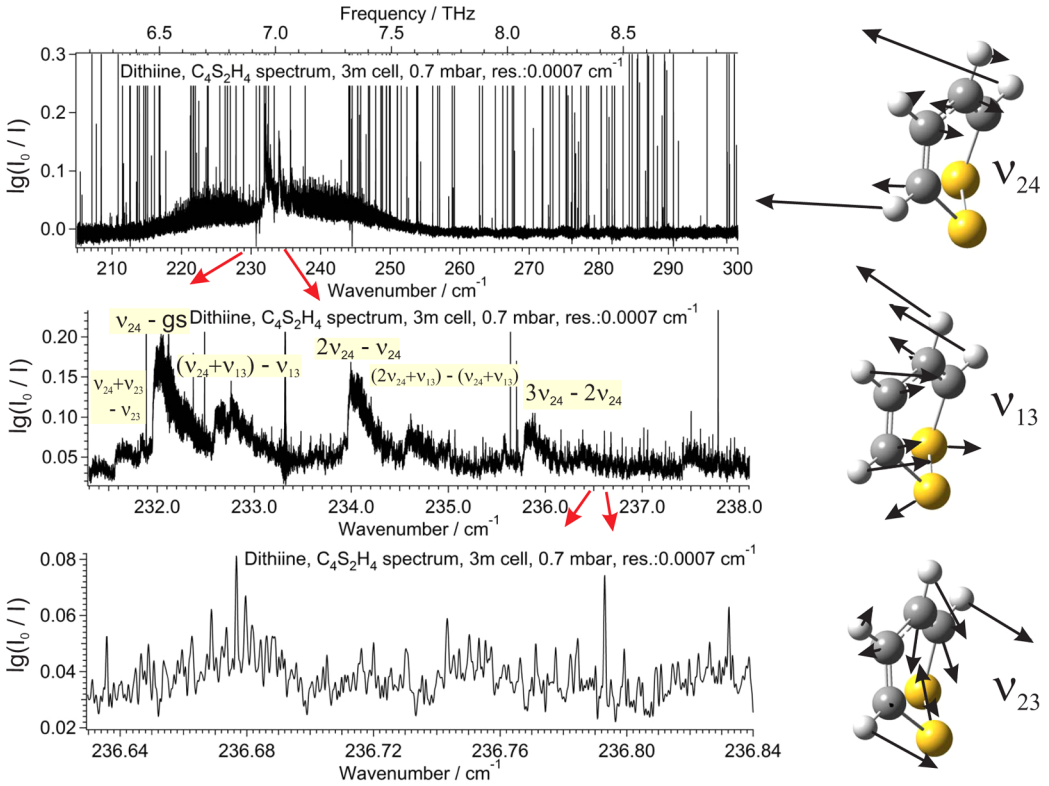

Figure 3. FIR spectrum of 1,2-dithiine ($C_4H_4S_2$) between 200 and 300 cm^{-1} using the Swiss Light Source (decadic absorbance $lg(I_0/I)$ is shown, conditions as given in the text). The numerous Q branches resulting from the fundamental and hot bands are visible in the experimental spectrum (see notation in the spectrum).

Table 1. Spectroscopic Constants in cm^{-1} of the Ground State of 1,2-Dithiine and the Other Bands in the *A* Reduction[a]

	ground state[b]	ν_{24}	$2\nu_{24}$	ν_{13}	$\nu_{13} + \nu_{24}$
$\tilde{\nu}_0/cm^{-1}$	0	231.952319 (10)	465.914320 (14)	x[c]	x + 232.579861 (33)
A/cm^{-1}	0.110955440	0.110991590 (10)	0.111021926 (13)	0.11083030 (31)	0.11086507 (30)
B/cm^{-1}	0.103499682	0.103540039 (14)	0.103578367 (55)	0.1033518 (26)	0.1033950 (24)
C/cm^{-1}	0.058573904	0.058644307 (11)	0.058709968 (72)	0.05847121 (57)	0.0585121 (60)
$\Delta_J/10^{-6}$ cm^{-1}	0.010662	0.0106844 (27)	0.0107001 (25)	0.010579 (59)	0.010626 (56)
$\Delta_{JK}/10^{-6}$ cm^{-1}	0.013599	0.013570 (11)	0.013570	0.013599	0.013599
$\Delta_K/10^{-6}$ cm^{-1}	−0.0059816	−0.0059514 (13)	−0.0059514	−0.0059816	−0.0059816
$\delta_J/10^{-6}$ cm^{-1}	0.0022477	0.0022436 (15)	0.002248 (15)	0.0022477	0.0022477
$\delta_K/10^{-6}$ cm^{-1}	0.015793	0.0159102 (35)	0.015983 (18)	0.015793	0.015793
N_{THz}		4318	1019		415
N_{GHz}		78		44	
d_{rms}(FIR)/cm^{-1}		0.00012	0.00013	0.00013	
J_{max} for fit		70	68	48	48
J_{max} assigned		70	68	48	48
K_{amax}		70	68	48	48
K_{cmax}		57	26	27	4

[a]The uncertainties are listed in parentheses in terms of 1σ in units of the last digits. [b]Fixed to the values from ref 41. [c]x is the unknown absolute value of the ν_{13} fundamental.

identified as P, R, and Q branches with $ee \leftrightarrow oe/eo \leftrightarrow oo$ transitions and $ee \leftrightarrow oo/eo \leftrightarrow oe$ transitions, respectively (e and o indicating whether K_a and K_c are even or odd). The lines have been assigned for $J \leq 70$, $K_a \leq 70$, and $K_c \leq 35$ for the *c*-type transitions and for $J \leq 70$, $K_a \leq 70$, and $K_c \leq 57$ for the *b*-type transitions. In the gigahertz spectra the *b*-type rotational transitions in the ν_{24} vibrational state have been assigned for J = 21 to 29 and K_a = 0 to 12 and K_c = 10 to 28. The hot band $2\nu_{24} \leftarrow \nu_{24}$ is centered at 233.96 cm^{-1} and consists mainly of *c*-type transitions that have been assigned for $J \leq 68$, $K_a \leq 68$, and $K_c \leq 26$. The *b*-type transitions have not yet been detected for this band. The third band assigned as $(\nu_{13} + \nu_{24}) \leftarrow \nu_{13}$ is centered at 232.96 cm^{-1} and consists of *b*-type transitions for $J \leq 48$, $K_a \leq 48$, and $K_c \leq 4$. The *b*-type rotational transitions in the ν_{13} vibrational state have been assigned for J = 21 to 27, K_a = 0 to 10, and K_c = 10 to 27. This band is interesting because it provides information about the puckering mode ν_{13}. A more detailed look at the Q branch region shows that there are three additional weak Q branches that can be assigned in a preliminary way without detailed rotational analysis but with

DOI: 10.1021/acs.jpclett.6b01674
J. Phys. Chem. Lett. 2016, 7, 3847−3853

Table 2. Comparison of Measured and Calculated Spectroscopic Parameters in cm^{-1} (α_i being defined in a standard way by $\alpha_v = (B_0 - B_{v_i})/v_i$)[a]

transition	$E_{exp}/(hc\ cm^{-1})$	$E_{anh}/(hc\ cm^{-1})$	$S/(km\ mol^{-1})$
$\nu_{13} \leftarrow gs$		177.3	0.03
$\nu_{24} \leftarrow gs$	231.95	236.3	12.29
$\nu_{23} \leftarrow gs$		315.4	0.23
$2\nu_{24} \leftarrow \nu_{24}$	233.91	238.36	7.77
$3\nu_{24} \leftarrow 2\nu_{24}$	235.8	240.4	3.64
$(\nu_{23} + \nu_{24}) \leftarrow \nu_{23}$	231.8	236.0	2.64
$(\nu_{13} + \nu_{24}) \leftarrow \nu_{13}$	232.58	237.23	5.18
$(\nu_{13} + 2\nu_{24}) \leftarrow (\nu_{13} + \nu_{24})$	234.6	239.29	3.29
$(2\nu_{13} + \nu_{24}) \leftarrow 2\nu_{13}$		238.2	2.21
transition−fundamental		$\Delta\tilde{\nu}_{exp}/cm^{-1}$	$\Delta\tilde{\nu}_{calc}/cm^{-1}$
$[2\nu_{24} \leftarrow \nu_{24}] - [\nu_{24} \leftarrow gs]$		1.96	2.06
$[3\nu_{24} \leftarrow 2\nu_{24}] - [\nu_{24} \leftarrow gs]$		3.8	4.11
$[(\nu_{13} + \nu_{24}) \leftarrow \nu_{13}] - [\nu_{24} \leftarrow gs]$		0.56	0.93
$[(2\nu_{13} + \nu_{24}) \leftarrow 2\nu_{13}] - [\nu_{24} \leftarrow gs]$			1.86
$[(\nu_{13} + 2\nu_{24}) \leftarrow (\nu_{13} + \nu_{24})\ ] - [\nu_{24} \leftarrow gs]$		2.7	2.98
$[(\nu_{23} + \nu_{24}) \leftarrow \nu_{23}] - [\nu_{24} \leftarrow gs]$		−0.15	−0.35
vibrational state	rot. const	$-\alpha_{exp}/cm^{-1}$	$-\alpha_{cal}/cm^{-1}$
ν_{24}	$A_{24} - A_0$	0.000037	0.000018
$2\nu_{24}$	$(A_{24,2} - A_0)/2$	0.000034	0.000018
ν_{24}	$B_{24} - B_0$	0.000040	0.000033
$2\nu_{24}$	$(B_{24,2} - B_0)/2$	0.000039	0.000033
ν_{24}	$C_{24} - C_0$	0.000070	0.000071
$2\nu_{24}$	$(C_{24,2} - C_0)/2$	0.000070	0.000071
ν_{13}	$A_{13} - A_0$	−0.000125	−0.000154
ν_{13}	$B_{13} - B_0$	−0.000150	−0.000157
ν_{13}	$C_{13} - C_0$	−0.000100	−0.000115

[a]Calculations were carried out at the B3LYP level of theory (see Supporting Information).

approximate positions estimated from the Q branches as $(\nu_{24} + \nu_{23}) \leftarrow \nu_{23}$ at 231.8 cm^{-1}, $(2\nu_{13} + \nu_{24}) \leftarrow (\nu_{13} + \nu_{24})$ at 234.6 cm^{-1}, and $3\nu_{24} \leftarrow 2\nu_{24}$ at 235.8 cm^{-1}.

The rovibrational analysis has been carried out with Watson's *A* reduced effective Hamiltonian[53] in the *I*^{r} representation up to sextic centrifugal distortion constants using our WANG program[54]

$$\begin{aligned}\hat{H}_{rot}^{v,v} = {} & A_v\hat{J}_z^2 + B_v\hat{J}_x^2 + C_v\hat{J}_y^2 - \Delta_J^v\hat{J}^4 - \Delta_{JK}^v\hat{J}^2\hat{J}_z^2 - \Delta_K^v\hat{J}_z^4 \\ & - \frac{1}{2}[(\delta_J^v\hat{J}^2 + \delta_K^v\hat{J}_z^2), (\hat{J}_+^2 + \hat{J}_-^2)]_+ + \Phi_J^v(\hat{J}^2)^3 \\ & + \Phi_{JK}^v(\hat{J}^2)^2\hat{J}_z^2 + \Phi_{KJ}^v\hat{J}^2\hat{J}_z^4 + \Phi_K^v\hat{J}_z^6 \\ & + \frac{1}{2}[(\phi_J^v(\hat{J}^2)^2 + \phi_{JK}^v\hat{J}^2\hat{J}_z^2 + \phi_K^v\hat{J}_z^4), (\hat{J}_+^2 + \hat{J}_-^2)]_+ \end{aligned} \quad (2)$$

Equation 2 defines the notation used for the parameters. The angular momentum operators are given by $\hat{J}^2 = \hat{J}_x^2 + \hat{J}_y^2 + \hat{J}_z^2$ and $\hat{J}_\pm = \hat{J}_x \pm i\hat{J}_y$. The *I*^{r} representation was chosen to reduce correlations during the fit. The spectroscopic constants were fitted for each band separately according to the *A* reduction.The Hamiltonian in eq 2 shows distortion terms through second order, but only terms through first order were retained in the final fit, as given in Table 1.

According to the calculated transition moments for the ν_{24} fundamental the *b*- and *c*-type absorption lines are predicted to be of similar intensity. Around 2000 *b*-type transitions and around 2300 *c*-type transitions have been used in the adjustment, where around 1500 lines are from coinciding nonsplit *c*-type and *b*-type transitions for $K_c \leq 11$. Pure *b*-type transitions (∼500) have been assigned. Pure *c*-type transitions (∼800) have been assigned in the entire spectrum. Overall, 4318 *b*- and *c*-type transitions for $J \leq 70$, $K_a \leq 70$, and $K_c \leq 57$ of the terahertz spectrum and the 78 *b*-type transitions from the gigahertz spectrum were used for the fit of the spectroscopic constants. There were no important perturbations observed in the spectrum, as the very small root-mean-square deviation d_{rms} = 0.00012 cm^{-1} for the terahertz lines indicates. The constants of the ground state have been held fixed to the values in Table 1, and the constants of ν_{24} have been adjusted in the least-squares analysis.

The adjustments of the constants for the $2\nu_{24}$ state have been carried out using the *b*-type transitions of the terahertz spectrum. Around 1000 lines have been used. During the adjustment of the constants of the lower level, the ν_{24} state has been held fixed to the values determined from the adjustment of the ν_{24} fundamental, which confirmed the assignment as $2\nu_{24} \leftarrow \nu_{24}$. The rotation−vibration α constants of the rotational constants of the ν_{24} vibrational state agree very well with the calculated values shown in Table 2 and confirm the assignment. The constants for $\nu_{13} + \nu_{24} \leftarrow \nu_{13}$ band have been adjusted using around 400 *b*-type transitions from the terahertz spectrum and the 44 rotational lines from the gigahertz spectrum. Therefore, some of the quartic constants have been fixed to the values of the ground state. The shifts of the center of the $2\nu_{24} \leftarrow \nu_{24}$ and $(\nu_{13} + \nu_{24}) \leftarrow \nu_{13}$ hot bands as shown in Table 2 confirm the assignments, too. In particular, the α constants of the ν_{13} state show a very good agreement with the calculated values. Also, the calculations indicate that the

DOI: 10.1021/acs.jpclett.6b01674
J. Phys. Chem. Lett. 2016, 7, 3847−3853

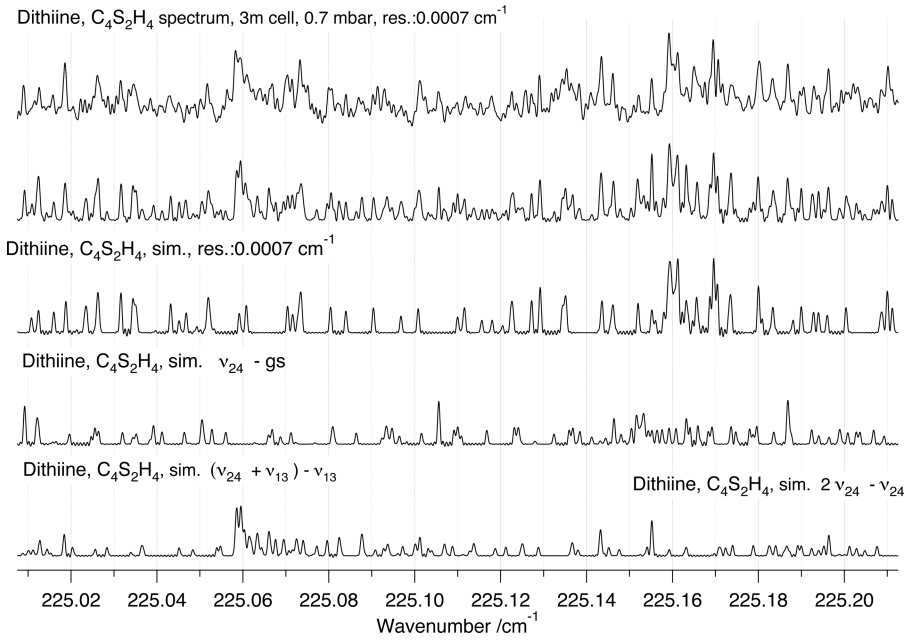

Figure 4. Comparison of the experimental spectrum (highest trace) of 1,2-dithiine measured at 295 K in the P branch region with a simulation of the ν_{24} fundamental (third trace), the $(\nu_{13}+\nu_{24}) \leftarrow \nu_{13}$ band (fourth trace), the $2\nu_{24} \leftarrow \nu_{24}$ band (lowest trace), and a sum of all three simulated bands (second trace). See parameters in the Figure. The decadic absorbances $\lg(I_0/I)$ are shown as a function of wavenumber, with maximum peak values of $\lg(I_0/I) = 0.06$ (3 m path length, 0.7 mbar, $\Delta\tilde{\nu} = 0.0007$ cm^{-1} from a convolution of an instrumental width of 0.0006 cm^{-1} with a Doppler width of 0.00026 cm^{-1}).

fundamentals ν_{23} and ν_{13} are too weak to be detected in our experiment.

A comparison of the measured spectrum with the simulated spectrum calculated with the parameters listed in Table 1 is shown in Figure 4 for the R and P branch regions. The upper trace shows the experimental spectrum, the second trace is the sum of all simulations, the third trace is the ν_{24} fundamental simulation, the fourth trace is the $\nu_{13} + \nu_{24} \leftarrow \nu_{13}$ simulation, and the lower trace is the $2\nu_{24} \leftarrow \nu_{24}$ simulation. As one can see, the agreement is very good. One recognizes the importance of hot bands to simulate the measured spectrum.

The ideal setup of the very stable synchrotron light source at the SLS with the currently highest resolution interferometric Fourier transform spectrometer is able to reduce noise levels in absorbance spectra to values by a factor of 100 lower than with conventional thermal sources. We have shown here that as a consequence of this advance high-resolution analyses are possible for the spectra of 1,2-dithiine in the very difficult far-infrared or terahertz range, for a chiral molecule that may at first sight seem exotic but is in fact one of the very few realistic candidates to measure the parity violating energy difference $\Delta_{pv}E$ between enantiomers, so far never detected.[4] The fundamental ν_{24} at 231.95 cm^{-1} agrees reasonably well with our theoretical results at the B3LYP level (236.3 cm^{-1}; see the Supporting Information). Also, the agreement between theory and the experimental anharmonic shifts of several hot band centers and the rotation vibration interaction constants is satisfactory. The rotational parameters for the ν_{13} and $\nu_{13} + \nu_{24}$ levels should be useful for the study of interactions of excited vibrational levels of ν_{13} with other vibrations, which will be relevant for future analyses, perhaps best starting with a reanalysis of the polyad associated with the ν_{22} fundamental (at 600 cm^{-1}, Figure 2).

The tunneling splitting $\Delta E_{\pm}$ ($v = 0$) in the ground state predicted at several levels of theory all consistently indicate that it is much smaller (by many orders of magnitude) than the predicted parity violating energy difference between the enantiomers, which is favorably large for a molecule containing no nucleus heavier than sulfur ($\Delta_{pv}E = 1.1 \times 10^{-11}$ (hc) cm^{-1}), leading to a relatively short "parity violating time" (1.5 s period) for which the initial evolution in the millisecond range should be detectable.[40,41] The present first high-resolution analysis and characterization of the spectrum of the low-frequency modes for this molecule provide an important step toward future analyses aiming at identifying combination levels at higher energy, which would be suitable for parity selection in the experiment on molecular parity violation.[40]

■ ASSOCIATED CONTENT

Supporting Information

The Supporting Information is available free of charge on the ACS Publications website at DOI: 10.1021/acs.jpclett.6b01674.

Tables of calculated vibrational wavenumbers, inversion potentials, tunneling splittings, anharmonic constants, and wavenumber shifts. Tables of measured and fitted line frequencies and wavenumbers with the assignments. (PDF)

■ AUTHOR INFORMATION

Corresponding Authors

*S.A.: E-mail: albert@ir.phys.chem.ethz.ch. Phone: +41446327918. Fax: +41446321021.

*M.Q.: E-mail: martin@quack.ch. Phone: +41446324421.

Notes

The authors declare no competing financial interest.

■ ACKNOWLEDGMENTS

We gratefully acknowledge help and support from, as well as discussions with Ľuboš Horný, Frithjof Nolting, and Robert

DOI: 10.1021/acs.jpclett.6b01674
J. Phys. Chem. Lett. 2016, 7, 3847−3853

Prentner. Our work is supported by an ERC advanced grant, the PSI/SLS, the Schweizerischer Nationalfonds, and the ETH Zürich. The research leading to these results has, in particular, also received funding from the European Union's Seventh Framework Programme (FP7/2007-20013) ERC grant agreement no. 290925 as well as the COST project MOLIM.

REFERENCES

(1) Hund, F. Zur Deutung der Molekelspektren. III. *Zeitschr. Physik* **1927**, *43*, 805−826.
(2) Merkt, F.; Quack, M. Molecular Quantum Mechanics and Molecular Spectra, Molecular Symmetry, and Interaction of Matter with Radiation. In *Handbook of High-Resolution Spectroscopy*; Quack, M., Merkt, F., Eds.; John Wiley & Sons, Ltd: Chichester, U.K., 2001; Vol *1*; Chapter 1, pp 1−55.
(3) Schatz, G. C., Ratner, M.A. *Quantum Mechanics in Chemistry*; Dover Books: Dover, NJ, 1993.
(4) Quack, M. Fundamental Symmetries and Symmetry Violations from High Resolution Spectroscopy. In *Handbook of High Resolution Spectroscopy*; Quack, M., Merkt, F., Eds.; John Wiley & Sons, Ltd: Chichester, U.K., 2011; Vol. *1*; Chapter 18, pp 659−722.
(5) Quack, M. Structure and Dynamics of Chiral Molecules. *Angew. Chem., Int. Ed. Engl.* **1989**, *28*, 571−586.
(6) Lee, T.; Yang, C. Question of parity conservation in weak interactions. *Phys. Rev.* **1956**, *104*, 254−258.
(7) Wu, C.; Ambler, E.; Hayward, R.; Hoppes, D.; Hudson, R. Experimental test of parity conservation in beta decay. *Phys. Rev.* **1957**, *105*, 1413−1415.
(8) Friedman, J. I.; Telegdi, V. L. Nuclear Emulsion Evidence for Parity Nonconservation in the Decay Chain $\pi^+-\nu^+-e^+$. *Phys. Rev.* **1957**, *105*, 1681−1682.
(9) Garwin, R. L.; Lederman, L. M.; Weinrich, M. Observations of the failure of conservation of parity and charge conjugation in meson decays - magnetic moment of the free muon. *Phys. Rev.* **1957**, *105*, 1415−1417.
(10) Schopper, H. Circular polarization of γ-rays: Further proof for parity failure in β decay. *Philos. Mag.* **1957**, *2*, 710−713.
(11) Weinberg, S. A model of leptons. *Phys. Rev. Lett.* **1967**, *19*, 1264−1266.
(12) McNaught, A. D.; Wilkinson, A. *IUPAC. Compendium of Chemical Terminology (the "Gold Book")*, 2nd ed.; Wiley Blackwell, 1997.
(13) Yamagata, Y. A hypothesis for the asymmetric appearance of biomolecules on earth. *J. Theor. Biol.* **1966**, *11*, 495−498.
(14) Rein, D. W. Some Remarks on Parity Violating Effects of Intramolecular Interactions. *J. Mol. Evol.* **1974**, *4*, 15−22.
(15) Mason, S. F. *Chemical Evolution: Origin of the Elements, Molecules, and Living Systems*; Clarendon Press: Oxford, 1991.
(16) Frank, P.; Bonner, W.; Zare, R. N. In *Chemistry for the 21st Century*; Keinan, E., Schechter, I., Eds.; Wiley-VCH: Weinheim, Germany, 2001; Chapter 11, pp 175−208.
(17) Quack, M. How Important is Parity Violation for Molecular and Biomolecular Chirality? *Angew. Chem., Int. Ed.* **2002**, *41*, 4618−4630.
(18) Quack, M. Molecular spectra, reaction dynamics, symmetries and life. *Chimia* **2003**, *57*, 147−160.
(19) Jortner, J. Conditions for the emergence of life on the early Earth: summary and reflections. *Philos. Trans. R. Soc., B* **2006**, *361*, 1877−1891.
(20) Quack, M. On Biomolecular Homochirality as a Quasi-Fossil of the Evolution of Life. *Advances in Chemical Physics* **2014**, *157*, 247−291.
(21) Berger, R. In *Relativistic Electronic Structure Theory*; Schwerdtfeger, P., Ed.; Elsevier: Amsterdam, 2004; Part 2, Chapter 4, pp 188−288.
(22) Quack, M.; Stohner, J.; Willeke, M. High-Resolution Spectroscopic Studies and Theory of Parity Violation in Chiral Molecules. *Annu. Rev. Phys. Chem.* **2008**, *59*, 741−769.
(23) Hegström, R. A.; Rein, D. W.; Sandars, P. G. H. Calculation of the Parity Non-Conserving Energy Difference between Mirror-Image Molecules. *J. Chem. Phys.* **1980**, *73*, 2329−2341.
(24) Mason, S. F.; Tranter, G. E. The parity-violating energy difference between enantiomeric molecules. *Mol. Phys.* **1984**, *53*, 1091−1111.
(25) Bakasov, A.; Ha, T.-K.; Quack, M. Ab Initio Calculation of Molecular Energies Including Parity Violating Interactions. In *Chemical Evolution: Physics of the Origin and Evolution of Life: Proceedings of the 4th Trieste Conference*; Kluwer Academic Publishers: Dordrecht, The Netherlands, 1995; pp 287−296.
(26) Lazzeretti, P.; Zanasi, R. On the calculation of parity-violating energies in hydrogen peroxide and hydrogen disulphide molecules within the random- phase approximation. *Chem. Phys. Lett.* **1997**, *279*, 349−354.
(27) Bakasov, A.; Ha, T. K.; Quack, M. Ab initio calculation of molecular energies including parity violating interactions. *J. Chem. Phys.* **1998**, *109*, 7263−7285.
(28) Bakasov, A.; Quack, M. Representation of parity violating potentials in molecular main chiral axis. *Chem. Phys. Lett.* **1999**, *303*, 547−557.
(29) Laerdahl, J. K.; Schwerdtfeger, P. Fully relativistic ab initio calculations of the energies of chiral molecules including parity-violating weak interactions. *Phys. Rev. A: At., Mol., Opt. Phys.* **1999**, *60*, 4439−4453.
(30) Berger, R.; Quack, M. Multiconfiguration linear response approach to the calculation of parity violating potentials in polyatomic molecules. *J. Chem. Phys.* **2000**, *112*, 3148−3158.
(31) Horný, L.; Quack, M. Computation of molecular parity violation using the coupled-cluster linear response approach. *Mol. Phys.* **2015**, *113*, 1768−1779.
(32) Letokhov, V. S. Difference of energy-levels of left and right molecules due to weak interactions. *Phys. Lett. A* **1975**, *53*, 275−276.
(33) Quack, M. On the Measurement of the Parity Violating Energy Difference Between Enantiomers. *Chem. Phys. Lett.* **1986**, *132*, 147−153.
(34) Quack, M. Frontiers in spectroscopy. *Faraday Discuss.* **2011**, *150*, 533−565.
(35) Bauder, A.; Beil, A.; Luckhaus, D.; Müller, F.; Quack, M. Combined high resolution infrared and microwave study of bromochlorofluoromethane. *J. Chem. Phys.* **1997**, *106*, 7558−7570.
(36) Daussy, C.; Marrel, T.; Amy-Klein, A.; Nguyen, C. T.; Bordé, C. J.; Chardonnet, C. Limit on the parity nonconserving energy difference between the enantiomers of a chiral molecule by laser spectroscopy. *Phys. Rev. Lett.* **1999**, *83*, 1554−1557.
(37) Schnell, M.; Küpper, J. Tailored molecular samples for precision spectroscopy experiments. *Faraday Discuss.* **2011**, *150*, 33.
(38) Tokunaga, S. K.; Stoeffler, C.; Auguste, F.; Shelkovnikov, A.; Daussy, C.; Amy-Klein, A.; Chardonnet, C.; Darquié, B. Probing weak force-induced parity violation by high-resolution mid-infrared molecular spectroscopy. *Mol. Phys.* **2013**, *111*, 2363−2373.
(39) Prentner, R.; Quack, M.; Stohner, J.; Willeke, M. Wavepacket Dynamics of the Axially Chiral Molecule ClOOCl under Coherent Radiative Excitation and Including Electroweak Parity Violation. *J. Phys. Chem. A* **2015**, *119*, 12805−12822.
(40) Dietiker, P.; Miloglyadov, E.; Quack, M.; Schneider, A.; Seyfang, G. Infrared laser induced population transfer and parity selection in $^{14}NH_3$: A proof of principle experiment towards detecting parity violation in chiral molecules. *J. Chem. Phys.* **2015**, *143*, 244305.
(41) Albert, S.; Bolotova, I.; Chen, Z.; Fábri, C.; Horný, L.; Quack, M.; Seyfang, G.; Zindel, D. High resolution GHz and THz (FTIR) spectroscopy and theory of parity violation and tunneling for 1,2-dithiine ($C_4H_4S_2$) as a candidate for measuring the parity violating energy difference between enantiomers of chiral molecules. *Phys. Chem. Chem. Phys.* **2016**, *18*, 21976−21993.
(42) Quack, M.; Willeke, M. Stereomutation Tunneling Switching Dynamics and Parity Violation in Chlorineperoxide Cl-O-O-Cl. *J. Phys. Chem. A* **2006**, *110*, 3338−3348.

DOI: 10.1021/acs.jpclett.6b01674
J. Phys. Chem. Lett. 2016, 7, 3847−3853

(43) Albert, S.; Albert, K. K.; Lerch, P.; Quack, M. Synchrotron-based highest resolution Fourier transform infrared spectroscopy of naphthalene ($C_{10}H_8$) and indole (C_8H_7N) and its application to astrophysical problems. *Faraday Discuss.* **2011**, *150*, 71−99.
(44) Albert, S.; Keppler, K.; Lerch, P.; Quack, M.; Wokaun, A. Synchrotron-based highest resolution FTIR spectroscopy of chlorobenzene. *J. Mol. Spectrosc.* **2015**, *315*, 92−101.
(45) Albert, S.; Lerch, P.; Prentner, R.; Quack, M. Tunneling and tunneling switching dynamics in phenol and its isotopomers from high resolution FTIR spectroscopy with synchrotron radiation in the THz range and theory. *Angew. Chem., Int. Ed.* **2013**, *52*, 346−349.
(46) Albert, S.; Lerch, P.; Quack, M. Synchrotron-Based Rotationally Resolved High-Resolution FTIR Spectroscopy of Azulene and the Unidentified Infrared Bands of Astronomy. *ChemPhysChem* **2013**, *14*, 3204−3208.
(47) Rothman, L. S.; et al. The HITRAN 2008 molecular spectroscopic database. *J. Quant. Spectrosc. Radiat. Transfer* **2009**, *110*, 533−572.
(48) Suter, M.; Quack, M. Line shape of amplitude or frequency-modulated spectral profiles including resonator distortions. *Appl. Opt.* **2015**, *54*, 4417−4431.
(49) Albert, S.; Keppler Albert, K.; Hollenstein, H.; Manca Tanner, C.; Quack, M. Fundamentals of Rotation-Vibration Spectra. In *Handbook of High-Resolution Spectroscopy*; Quack, M., Merkt, F., Eds.; John Wiley & Sons, Ltd: Chichester, U.K., 2011; Vol. *1*; Chapter 3, pp 117−173.
(50) Frisch, M. J.; et al. *Gaussian 09*, revision E.01; Gaussian, Inc.: Wallingford, CT, 2009.
(51) Albert, S.; Winnewisser, M.; Winnewisser, B. P. Networks of Anharmonic Resonance Systems in the Rovibrational Overtone Spectra of the Quasilinear Molecule HCNO. *Ber. Bunsenges. Phys. Chem.* **1996**, *100*, 1876−1896.
(52) Albert, S.; Winnewisser, M.; Winnewisser, B. P. The ν_1, ν_2, $2\nu_3$, $\nu_2+\nu_3$ Band Systems and the Overtone Region of HCNO above 4000 cm^{-1}: Networks of Resonance Systems. *Ber. Bunsenges. Phys. Chem.* **1997**, *101*, 1165−1186.
(53) Watson, J. K. G. In *Vibrational Spectra and Structure*; Durig, J., Ed.; Elsevier: Amsterdam, 1978; Vol. *6*, pp 1−89.
(54) Luckhaus, D.; Quack, M. The far infrared pure rotational spectrum and the Coriolis coupling between ν_3 and ν_8 in $CH^{35}ClF_2$. *Mol. Phys.* **1989**, *68*, 745−758.

DOI: 10.1021/acs.jpclett.6b01674
J. Phys. Chem. Lett. 2016, 7, 3847−3853